Electric properties of the low-lying excited states of benzonitrile: geometry relaxation and solvent effects

ARTICLE *in* THEORETICAL CHEMISTRY ACCOUNTS · JUNE 2015

Impact Factor: 2.23 · DOI: 10.1007/s00214-015-1678-7

3 AUTHORS:

Miroslav Medved'

Univerzita Mateja Bela v Banskej Bystrici

31 PUBLICATIONS **385** CITATIONS

SEE PROFILE

Šimon Budzák

University of Nantes

19 PUBLICATIONS **93** CITATIONS

SEE PROFILE

Tadeusz Pluta

University of Silesia in Katowice

19 PUBLICATIONS **312** CITATIONS

SEE PROFILE

Theor Chem Acc (2015) 134:78
DOI 10.1007/s00214-015-1678-7

REGULAR ARTICLE

Electric properties of the low-lying excited states of benzonitrile: geometry relaxation and solvent effects

Miroslav Medveď[1] · Šimon Budzák[1] · Tadeusz Pluta[2]

Received: 10 February 2015 / Accepted: 19 May 2015

Abstract Accurate calculations of the dipole moment and the polarizability for the ground and two lowest singlet and triplet excited states of benzonitrile (BN) have been performed by a variety of wave function and density functional theory (DFT) methods. Changes in molecular properties upon the electron excitation strongly depend on the character of an excited state. The vertical dipole moment change and the excess polarizability for the 1^1B state are smaller than those for the 2^1A state. In order to estimate adiabatic excited-state properties, corresponding relaxed geometries have been obtained using the PBE0 functional with the aug-cc-pVTZ basis set. The excited-state property values obtained with the long-range exchange corrected DFT methods are in general closer to the coupled cluster (CC) results, although the hybrid DFTs also provide reasonable predictions. Our CCSD adiabatic excess dipole moment value for the 1^1B state equal to 0.11 D is in excellent agreement with the experimental value. The 2^1A state appears to be more sensitive to selected method due to an important role of double-excitation effects. Solvent effects on dipole moment and polarizability of BN molecule in its ground and excited states were evaluated using both LR and cLR methods combined with the (TD-)CAMB3LYP/POL approach.

✉ Miroslav Medveď
miroslav.medved@umb.sk

[1] Department of Chemistry, Faculty of Natural Sciences, Matej Bel University, Tajovského 40, 97400 Banská Bystrica, Slovak Republic

[2] Institute of Chemistry, University of Silesia, Szkolna 9, 40007 Katowice, Poland

Keywords Excited states · Dipole moment · Polarizability · TD-DFT · Solvent effects

1 Introduction

Electric properties of molecules in excited electronic states are far less known and less frequently studied than their ground-state counterparts despite the fact that these properties are of growing interest, e.g., in studying materials with large nonlinear optical response [1, 2]. The knowledge of electric dipole moments and polarizability of excited states, often expressed as the difference between the excited- and ground-state property, i.e., excess dipole moment ($\Delta\mu$) and excess polarizability ($\Delta\alpha$), is also vital for better understanding of processes like the exciton localization/delocalization in conjugated porphyrin oligomers [3].

Documented computational attempts to determine excited-state electric properties are rather limited. Only electric excess properties of small systems such as water molecule [4, 5], hydrogen sulfide [6] and acetone [7] were examined thoroughly using advanced quantum chemical methods including electron correlation effects and the multi-configurational character of the excited states like CASSCF/CASPT2 [4, 6] or coupled cluster (CC) [7] methods. The main conclusion that can be drawn from these calculations is that the electric excess properties are strongly state-dependent and can reach high values.

The main sources of experimental data on excited-state dipole moment and polarizability are the Stark effect or electroabsorption/electrofluorescence measurements where the shift of the absorption/fluorescence band is observed as a function of an applied electric field. The measurements can be carried out for molecules in gas phase, in fluid solution, in a polymer film or in a frozen glass. The latter has

Published online: 28 May 2015

been successfully used for larger systems of biological interest, for reviews, see, e.g., [8, 9].

There are only few computational studies on the excess dipole moment and polarizability of medium-sized and/or larger molecules carried out in connection with the electroabsorption experiments [10]. The results reported there rely on the semiempirical and Hartree–Fock descriptions of the electronic structure of the studied excited states and therefore cannot be regarded as trustworthy because of the inherent approximate nature of the underlying wave function. The description of the electronic structure of excited states based on the modern density functional theory (DFT) calculations seems to be much better choice. In the last decade, time-dependent DFT (TDDFT) has become the method of choice for evaluation of the electronic excitation energies, especially for larger molecules where advanced wave function-based methods cannot be applied (for recent reviews on TDDFT, see, e.g., [11]). The success of TDDFT depends critically on the choice of the functional employed, and it was shown that the combination with the standard numerical differentiation with respect to the external electric field also known as the finite field (FF) technique leads to reliable determination of the electric excess properties of uracil [12]. Previously, similar approach combining linear response (LR) version of TDDFT and the FF technique was used by Grozema et al. [13, 14]. Before the proposed combination becomes a dependable and robust tool, more tests and comparisons with accurate wave function-based methods and experimental data are needed.

The goal of the present study is to determine the excess dipole moment ($\Delta\mu$) and the excess polarizability ($\Delta\alpha$) for the lowest singlet excited state of the benzonitrile (BN) molecule, for which experimental data on $\Delta\mu$ are available [15, 16]. We also investigate the second singlet excited state as well as two lowest triplet excited states. Let us note that there is very little experimental information on excess properties of triplet states. Since these states are not accessible by direct excitation from the ground state, no triplet data are available from electroabsorption measurements. Long-living triplet states can be studied using the flash photolysis time-resolved microwave conductivity (FP-TRMC) technique provided that the quantum yield for intersystem crossing is large enough [17]. Therefore, quantum chemistry methods can provide a useful insight to these quantities.

The performance of DFT methods including a representative set of exchange–correlation (XC) functionals: standard BLYP [18, 19], hybrid functionals B3LYP [20, 21], PBE0 [22], coulomb-attenuated (CAM) B3LYP [23], long-range corrected ωB97XD [24], long-range corrected BLYP [25] and recently introduced highly parametrized M06-2X [26] functional in the excess property calculations, was assessed by comparison with the experimental data and/or CC results at the CCSD (CCSD(T)) [27] and CC2 [28] levels. Possible static correlation effects have been addressed by the CASSCF method [27] as well as the CASPT2 approach [28, 29] including dynamic electron correlation effects up to the second order of the perturbation theory. Since the majority of experimental data on electroabsorption comes from measurements done in solution, we performed calculations in the explicit presence of some popular solvents within the framework of the polarizable continuum model (PCM) in the LR and corrected LR formalism (cLR) realizations (vide infra).

2 Computational details

The ground-state geometry of the BN molecule has been optimized using the B3LYP functional and the *aug*-cc-pVTZ basis set [30]. The optimized structure has the C_{2v} symmetry. If the excited-state calculations are performed with the ground-state geometries, they correspond to absorbtion (or electroabsorption if the external electric field is present). On the other hand, electroemission bands correspond to transitions from geometrically relaxed excited states; therefore, geometry optimization of the excited states is needed. The properties corresponding to the former are referred to as *vertical* ones, while those obtained for the latter are called *adiabatic*. In order to obtain relaxed excited-state geometries, we have used the PBE0 functional which was shown to give reliable structures provided that one does not inspect the states where the self-interaction error plays a significant role (e.g., charge transfer or Rydberg states) [31]. As in the case of the ground state, the *aug*-cc-pVTZ basis set was applied. The most important structural feature of all the examined low-lying excited states is that the molecule retains the C_{2v} symmetry. The structural data of the ground as well as excited states are presented in Fig. 1.

In all calculations of properties reported here, we have used the Sadlej POL basis [32] which provides sufficient flexibility to yield accurate values of electric properties [33]. Since our interest is limited to valence excited states, there is no need to enlarge the basis set or to augment it with functions designed for characterization of the Rydberg transitions. Nevertheless, we have compared vertical excitation energies calculated by CC2/POL with larger CC2/aug-cc-pVTZ calculation. The maximum difference between both approaches was 0.036 eV (for the 2^1A state), with average <0.02 eV. We note that with the POL basis set the total number of basis functions was only half of the aug-cc-pVTZ size.

We have applied several TDDFT methods to calculate excitation energies for the two lowest singlet and triplet excited states of BN. The formalism and its implementations are well described in the literature, see, e.g., [11];

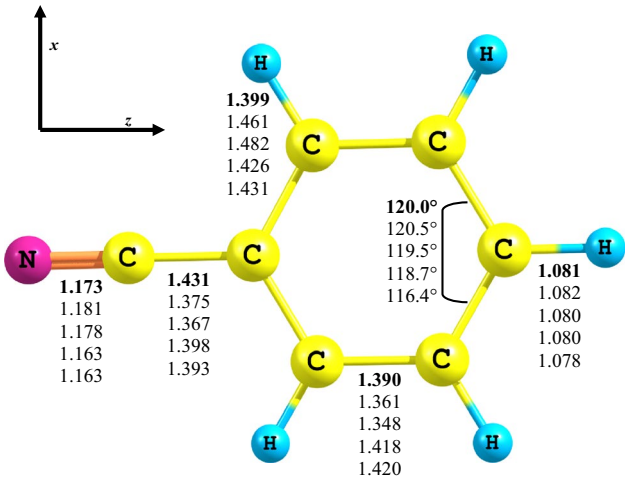

Fig. 1 Selected bond lengths and angle in benzonitrile molecule, in optimized ground state (*bold*) and excited states ($^1A_1$, $^3A_1$, $^1B_1$, $^3B_1$). Bond lengths are in 10^{-10} m and bond angle in deg

therefore, there is no need to present it here. As already mentioned, due to a favorable balance between computational cost and accuracy, TDDFT has become the method of choice for describing excited states of medium-sized molecules. However, since it is a single excitations approach, its applicability for excitations dominated by two or more electron interactions is severely limited. Charge transfer excitations as well as Rydberg states are also poorly described by standard (LDA, GGA and hybrid) TDDFT methods regardless of the choice of the exchange–correlation functional (XCF). The last two problems attributed to TDDFT can be resolved by using an asymptotically corrected exchange part of the electron interaction in the XCF. From practical experience, asymptotically corrected XCFs with 20–25 % of HF exchange in the short-range (SR) region lead to the most accurate results for singly excited states of finite systems [11, 34]. Based on this knowledge, we have chosen three long-range (LR) corrected XCFs: (1) computationally the least demanding LC-BLYP (with the range separation factor equal to 0.33) [35] applying pure Becke's exchange functional [18] for the SR interaction region; (2) CAM-B3LYP from Handy et al. [23] derived from B3LYP and thus mixing 20 % of the SR-HF exchange; and (3) ωB97XD proposed by Head-Gordon [24] which contains about 22 % of SR-HF exchange. Since valence excitations in BN are not expected to have typical long-range charge transfer character, standard XCFs are worth testing. We used in our study two hybrid XCFs, namely B3LYP and PBE0, which were successfully used for evaluation of excitation energies in several benchmark studies [34, 36]. Since previous works on simulating electronic spectra [37] have also shown promising performance of highly parameterized M06-2X functional which includes relatively high percentage (54 %) of HF exchange [26], this XCF was also included in our study.

When looking for a systematic inclusion of the electron correlation effects for excited-state calculations, one can rely on the hierarchy of CC methods. Computational demands and applicability of the LR version of the CC formalism [38] allowed us to apply the hierarchy up to CC with single and double excitations. The perturbative treatment of triple excitations within the CCSD(T) method was applied for electric properties of the ground state. Due to current implementation in Dalton program [39], we were limited to CC2 (second-order approximation of the CC response theory) [40] and CCSD (without orbital relaxation) for the properties of the singlet excited states. In the case of triplet states, we report the CC2 and CCSD excitation energies obtained by means of the response theory together with the FF CCSD and CCSD(T) dipole moment values. We note that in the FF calculations molecular orbitals are relaxed.

In order to assess the static electron correlation effects on properties of BN, we also applied a state specific version of the complete active space self-consistent field (SS-CASSCF) method. Although CASSCF enables rather general treatment of various excited states, it depends on the choice of active space. Since we are interested in the two lowest excited states, which are of π–π^* character, our active space includes ten electrons in ten active π orbitals, which cover two π orbitals from cyano group, all three π orbitals from benzene and respective antibonding π^* orbitals. Let us note that Zilberg and Haas in their work [41] relied on the CAS (8,8) which did not include the lowest π orbital (nor its antibonding counterpart) from benzene. In another work, Sobolewski et al. [42] used the CAS (10, 10), i.e., the same size as in our work, but since they were predominantly interested in the n–π^* excitations, instead of the lowest π orbital they included the lone pair orbital on nitrogen. However, it can be expected that this orbital does not play a significant role in π–π^* transitions. In order to include dynamic electron correlation effects, the CASPT2 method [28, 29] has been applied.

Most of the reported dipole moment and polarizability values have been determined by the standard FF method using the Romberg procedure [43, 44]. The minimum external electric field (F_0) was set to 2×10^{-4} a.u. (1 a.u. = 5.1422 × 1011 V m^{-1}), and the other field amplitudes were given by $\pm 2^k F_0$ with $k = 1, 2, \ldots, 6$. In the present study, we have limited our interest to the second-order property; therefore, we have not encountered any particular problems with the convergence and numerical stability. Application of the electric field in x and y direction (see Fig. 1) lowers the molecular symmetry and hence leads to mixing between states originally of different

symmetry. Therefore, in the case of CCSD (triplet states) and CCSD(T), we report only the excess dipole moment values.

Solvent effects on excitation energies and electric properties were taken into account by the polarizable continuum model (IEF-PCM) [45, 46]. This model has been successfully used for evaluating molecular properties in solvent [47–49]. However, it is necessary to underline that continuum models are not suitable for obtaining reliable values if the solute–solvent interactions include hydrogen bonds (see, e.g., [50]). Since we focus on vertical excitations, non-equilibrium LR [51, 52] as well as corrected LR [53] model has been applied. These methods differ by the treatment of the change in the solvent polarization when going from the ground to the excited state, in the LR scheme, the transition densities are used to determine the change in charges on the PCM cavity surface, while in the cLR model the one-particle TD-DFT density matrix, that accounts for the orbital relaxation contribution, is used in a perturbation approach. In all PCM calculation, the CAM-B3LYP functional was used to evaluate the electric properties.

We have carried out our computations using several software packages. Gamess [54, 55] was used to optimize all geometries and also for CCSD(T) calculations. GAUSSIAN 09 [56] was used for DFT as well as for all solvent PCM calculations. CC2, CCSD and CASSCF results have been obtained with the Dalton code [39]. The CASPT2 calculations have been performed with the MOLCAS 7.6 program [57].

Table 1 Electric properties of the ground state of benzonitrile obtained with the Sadlej's POL basis sets using the optimized B3LYP/aug-cc-pVTZ geometry

Method	μ[a]	α_{xx}	α_{yy}	α_{zz}	α_{av}
HF	5.071	50.85	84.39	117.96	84.40
MP2	4.486	51.08	86.50	119.86	85.81
B3LYP	4.753	50.43	87.30	125.84	87.86
CAMB	4.791	50.14	86.36	122.74	86.41
PBE0	4.748	49.79	86.13	124.02	86.65
BLYP	4.666	51.26	89.20	130.10	90.19
LC-BLYP	4.773	50.50	86.80	122.37	86.56
ωB97XD	4.773	50.59	86.13	122.59	86.44
M06-2X	4.749	49.98	85.65	121.55	85.73
CASSCF[b]	4.427	48.26	79.26	106.07	77.87
CASPT2[b]	4.422				
CCSD	4.525	50.97	86.40	119.65	85.68
CCSD(T)	4.483	50.60	85.00	118.60	84.73
Experimental data					
Lide [58]	4.14				
Lide [60]	4.18				
Borst et al. [15]	4.48				
Wohlfart et al. [59]	4.5152				

The dipole moment values are given in debyes; polarizability values are in given a.u.

[a] The length of the dipole moment vector

[b] The active space in the CASSCF and CASPT2 calculations includes ten electrons in ten active π orbitals (see text for details)

3 Results and discussion

3.1 Ground-state properties of BN in the gas phase

Although in our study we focus on the excited-state properties, we start our discussion with the ground-state properties. In Table 1, we report the dipole moment (μ) and the polarizability (α) values of BN in its ground state evaluated by various DFT- and WF-based methods. As far as the experimental μ_g values, we see that they range from 4.14 up to 4.52 D [15, 58–60]. Nevertheless, we consider the most recent value of 4.5152 D obtained by measuring the Stark shift of selected hyperfine transitions using the Fourier transform microwave spectroscopy by Wohlfart et al. [59] as the most accurate. This value is very close to that reported by Borst et al. (4.48 D) determined from Stark shift measurements of the rotationally resolved laser-induced fluorescence spectrum [15]. A comparison of our theoretical results with these values shows excellent agreement for both CCSD (4.525 D) and CCSD(T) (4.483 D) methods. The MP2 value (4.486 D) appears to be as accurate as the CC results. The role of electron correlation is evident here. On the other hand, all applied hybrid and LRC-DFT methods slightly overshoot the dipole moment value (by ca. 0.20–0.25 D). Although the BLYP result is closer to the reference value, the reliability of the result is under question due to its failure in prediction of α (see below). Let us make a short remark on the comparison of theoretical and experimental dipole moment data. Since the experimental values are obtained from analyses of fluorescence spectra, the geometry effects due to relaxation of the measured excited state could affect the final ground-state dipole moment value. In order to estimate this effect, we have calculated μ_g of BN at the CCSD level using the relaxed geometry of the first singlet excited state (1^1B) revealing the value 4.473 D. According to this result, the error due to the excited-state relaxation effects is about 0.05 D.

To our best knowledge, the gas-phase α of BN is not known experimentally. The experimental measurements of the Kerr effect in nonpolar solvents such as benzene and CCl_4 lead to the values of α_{av} in the range 83.0–84.4 a.u. [60–62], which are in reasonable agreement with the value 81.5 a.u. obtained by Alvarado et al. [63] using the refractometric method and CCl_4 as a solvent. Although our

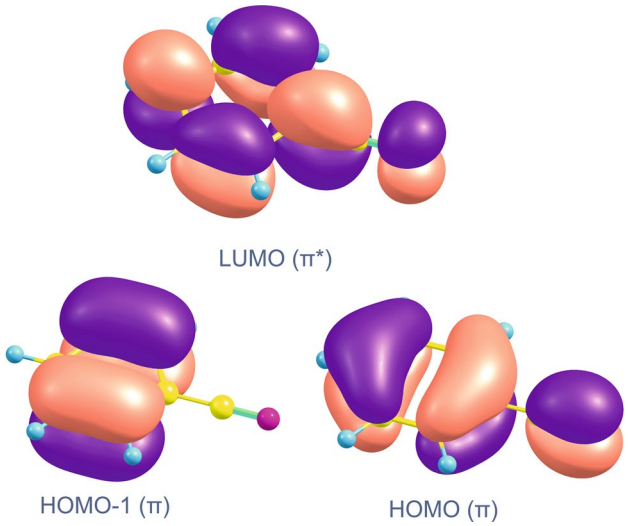

Fig. 2 Frontier orbitals in benzonitrile

theoretical gas-phase values cannot be directly compared to these experiments, they appear to be fairly consistent. Taking the CCSD(T) value (84.73 a.u.) as a reference value for other calculations, we can observe very good performance of MP2 and CCSD methods. Hybrid and LRC-DFT methods slightly (by ca. 1–2 a.u.) overshoot the reference value, M06-2X giving the closest value (85.73). On the contrary, the overestimation by BLYP is close to 5.5 a.u., i.e., more than 6 %.

3.2 Gas-phase excited-state structures and excitation energies

The two lowest singlet excited states belong to the B_1 (B in C_2) and A_1 (A in C_2) irreducible representations of the C_{2v} symmetry. We refer to these states as 1^1B and 2^1A, respectively. Their nature can be expressed in terms of the frontier orbitals (see Fig. 2), which are of π (π^*) character. While the former can predominantly be described as the electron excitation from the HOMO-1 to LUMO, in the latter an electron excites from HOMO to LUMO. Conversely, the two lowest triplet states show up the reverse ordering, i.e., the 1^3A state appears to be below the 1^3B state.

In order to calculate adiabatic excited-state properties, we have optimized geometries of the excited states of BN (see Fig. 1). In line with analysis of the geometry changes due to singlet excitations by Zilberg and Haas [41] at the CASSCF/DZV level, the structure of the 1^1B state determined by PBE0/*aug*-cc-pVTZ is very similar to that of the analogous 1^1B_{2u} state of benzene, i.e., the benzene ring remains almost a perfect hexagon as in the ground state, with a small increase in the CC bond length (from about 1.39 to 1.42 Å). This fact indicates that the 1^1B state can be described as a locally excited state in which excitation occurs within the benzene moiety. The local character of the excitation is in line with a very small change in the dipole moment and polarizability (see further) and also with the so-called Λ value corresponding to an overlap of the ground- and excited-state densities as defined by Tozer et al. [64], which is equal to 0.63 for the 1^1B state. Let us recall that the parameter Λ was proposed to indicate the charge transfer or Rydberg character of excitations, which are rather problematic case for standard (i.e., pure, GGA and hybrid) DFT methods. Although the 2^1A state can also be characterized as local (the Λ parameter is equal to 0.85, i.e., it is even larger than that for the 1^1B state), it has the quinoid structure, in which the two central CC bonds of the benzene ring are shorter by about 0.1 Å than the other four CC bonds. In addition, the CC bond between the benzene ring and the cyano group shortens significantly compared with the ground state. The more pronounced structural changes upon the excitation to the 2^1A state can be explained in terms of the shapes of HOMO and LUMO (Fig. 2). While the HOMO has nodal planes crossing the two central CC bonds of the benzene ring as well as the CC bond between the benzene ring and the CN group, the increased population of the LUMO (π^*) leads to strengthening these bonds. The changes in population of the frontier orbitals are reflected in partial increase in the bond orders of these bonds (from 1.08 to 1.23 and from 1.45 to 1.53, respectively) as obtained from the bond index matrix in the natural atomic orbital (NAO) basis [65] at the M06-2X/*aug*-cc-pVTZ level. The structures of the triplet states are similar to their singlet counterparts with even more pronounced quinoid character of the 1^3A state.

In Tables 2 and 3, we report vertical electronic excitation energies for the lowest singlet and triplet states, respectively. Although the Sadlej POL basis was not originally designed for excitation energy calculations, its capability to provide reasonable estimates obviously needs to be addressed when discussing excited-state properties. Tables 2 and 3 show that at the CC2 level the vertical excitation energies calculated by using the POL basis set differ from the aug-cc-pVTZ results at most by 0.04 eV. It can be seen that for the 1^1B state as well as for both triplet states, all applied methods give more or less consistent results. On the other hand, in the case of the 2^1A state, the CASSCF method predicts too high excitation energy (7.41 eV) compared with other methods, although the inclusion of the dynamic correlation effects at the CASPT2 level brings the result (6.28 eV) much closer to the CCSD value (6.12 eV).

Adiabatic electronic excitation energies are reported in Tables 4 and 5. Experimental value for the 1^1B state (4.53 eV) has been obtained from the high-resolution fluorescence excitation of BN in the gas phase by Borst et al. [66]. We note that according to the paper by Winter et al.

Table 2 Vertical excitation energies (in eV), dipole moment and its excess (in D) and polarizability and its excess (in a.u.) of the low-lying singlet excited states of benzonitrile obtained with Sadlej's POL basis sets

State	1^1B					2^1A				
	ΔE	μ	$\Delta\mu$	α_{av}	$\Delta\alpha$	ΔE	μ	$\Delta\mu$	α_{av}	$\Delta\alpha$
B3LYP	5.04	4.999	0.246	106.0	18.2	5.46	4.422	−0.332	125.1	37.3
CAMB	5.20	5.061	0.269	98.5	12.0	5.63	4.714	−0.077	113.7	27.3
PBE0	5.14	5.012	0.264	103.0	16.3	5.56	4.443	−0.305	121.0	34.4
BLYP	4.76	4.704	0.039	117.0	26.8	5.24	3.985	−0.680	142.5	52.3
LC-BLYP	5.19	4.981	0.208	95.7	9.1	5.72	4.816	0.042	112.2	25.6
ωB97XD	5.22	5.058	0.285	97.9	11.4	5.67	4.711	−0.062	113.1	26.7
M06-2X	5.28	4.981	0.231	97.7	11.9	5.76	4.678	−0.072	116.7	31.0
CASSCF	4.84	4.397	−0.030			7.41	7.259	2.832		
CASPT2	4.83	4.401	−0.021			6.28	7.243	2.821		
CC2[a]	5.06 (5.04)	4.542	0.107	100.5	11.3	6.05 (6.02)	4.809	0.374	137.6	48.4
CCSD	5.01	4.571	0.046	92.0	6.4	6.12	4.911	0.386	125.5	39.8
Previous works										
CASSCF/DZV[b]	4.96	4.20				7.63	7.11			
CASPT2/DZV[b]	4.64					6.24				

[a] The *aug*-cc-pVTZ results are given in parentheses

[b] Sobolewski et al. [42]. For details, see text

Table 3 Vertical excitation energies (in eV), dipole moment and its excess (in D) and polarizability and its excess (in a.u.) of the low-lying triplet excited states of benzonitrile obtained with Sadlej's POL basis sets

State	1^3A					1^3B				
	ΔE	μ	$\Delta\mu$	α_{av}	$\Delta\alpha$	ΔE	μ	$\Delta\mu$	α_{av}	$\Delta\alpha$
B3LYP	3.42	4.331	−0.423	92.5	4.6	4.30	6.199	1.446	107.4	19.6
CAMB	3.22	4.418	−0.373	86.4	0.0	4.41	6.190	1.399	105.0	18.6
PBE0	3.27	4.306	−0.442	88.6	1.9	4.32	6.161	1.413	105.9	19.2
BLYP	3.57	4.208	−0.458	102.3	12.1	4.17	6.224	1.558	113.7	23.5
LC-BLYP	3.35	4.508	−0.265	87.7	1.1	4.46	6.166	1.393	102.7	16.1
ωB97XD	3.41	4.435	−0.338	88.4	1.9	4.47	6.183	1.410	103.5	17.1
M06-2X	3.87	4.536	−0.213	94.6	8.9	4.64	6.111	1.362	101.1	15.4
CASSCF	4.84	4.314	−0.113			3.69	4.704	0.227		
CASPT2	3.92	4.919	0.497			4.59	5.837	1.415		
CC2[a]	4.06 (4.08)					4.86 (4.84)				
CC3	3.86					4.65				
CCSD	3.72	4.308	−0.217			4.72	5.968	1.443		
CCSD(T)		4.359	−0.125				5.828	1.344		

[a] The *aug*-cc-pVTZ results are given in parentheses

[67] the zero-point vibrational (ZPV) correction to the 0–0 transition energy (not accounted for in our calculations) evaluated for the 1^1B state is about −0.12 eV. It can be seen that our theoretical excitation values obtained with the correlation WF-based methods are about 0.3 eV higher than the experimental value and thus by adding the ZPV correction from [67] we achieve very good agreement with the experiment. Let us mention that Zilberg and Haas [41] obtained somewhat lower value (4.27 eV) at the CASPT2 level, but they used smaller active space and also smaller (DZV) basis set. Hybrid and LRC-DFT estimates being slightly higher (by ca. 0.1–0.2 eV) than the CC2 and CCSD values are close to each other, which could be expected for the local electronic transition. Similar performance of the hybrid and LRC-DFT methods with respect to CCSD has been observed in the case of adiabatic excitation energy for the 1^3B state as well as for their vertical counterparts. The excitation energy of the 2^1A state was found to be slightly more sensitive to the applied method. Nevertheless, the hybrid and LRC-DFT values (underestimating the CCSD value by about 0.4–0.5 eV) are still fairly close to each other (within 0.2 eV), which is again consistent with the large value (0.85) of the Λ parameter.

Table 4 Adiabatic excitation energies (in eV), dipole moment and its excess (in D) and polarizability and its excess (in a.u.) of the low-lying singlet excited states of benzonitrile

State	1^1B					2^1A				
	ΔE	μ	$\Delta\mu$	α_{av}	$\Delta\alpha$	ΔE	μ	$\Delta\mu$	α_{av}	$\Delta\alpha$
B3LYP	4.91	5.106	0.353	105.0	17.2	5.20	4.391	−0.363	112.8	25.0
CAMB	5.11	5.156	0.365	99.2	12.8	5.37	4.661	−0.130	94.0	7.6
PBE0	5.03	5.122	0.374	102.4	15.7	5.31	4.408	−0.340	109.0	22.4
BLYP	4.59	4.851	0.185	113.0	22.8	4.97	4.086	−0.580	123.3	33.1
LC-BLYP	5.09	5.075	0.302	96.6	10.1	5.44	4.778	0.006	105.8	19.2
ωB97XD	5.11	5.146	0.374	98.5	12.1	5.40	4.650	−0.123	102.1	15.7
M06-2X	5.16	5.085	0.336	98.1	12.4	5.47	4.640	−0.110	105.8	20.0
CASSCF	4.67	4.385	−0.042			6.97	3.446	−0.981		
CASPT2	4.65	4.376	−0.046			6.55	3.491	−0.931		
CC2	4.89	4.623	0.187	98.7	9.5	5.73	4.571	0.135	130.5	41.3
CCSD	4.85	4.633	0.108	93.1	7.4	5.87	4.890	0.365	122.2	36.5
Previous works										
CASSCF/DZV[a]	4.55	4.4	−0.1			6.60	4.0	−0.5		
CASPT2/DZV[a]	4.27					6.35				
Experimental data	4.53[b]	4.57[c]	0.09							
		4.42[d]	0.24							

Relaxed geometries have been obtained with PBE0 using the aug-cc-pVTZ basis sets

[a] Zilberg and Haas [41]. For details, see text

[b] Borst et al. [66]

[c] Borst et al. [15]

[d] Kawski et al. [16]

Table 5 Adiabatic excitation energies (in eV), dipole moment and its excess (in D) and polarizability and its excess (in a.u.) of the low-lying triplet excited states of benzonitrile

State	1^3A					1^3B				
	ΔE	μ	$\Delta\mu$	α_{av}	$\Delta\alpha$	ΔE	μ	$\Delta\mu$	α_{av}	$\Delta\alpha$
B3LYP	3.00	4.259	−0.495	92.3	4.4	4.55	6.573	1.819	105.4	17.5
CAMB	2.82	4.258	−0.533	87.6	1.1	4.27	6.590	1.798	104.7	18.3
PBE0	2.89	4.198	−0.550	89.1	2.5	4.16	6.560	1.812	104.3	17.7
BLYP	3.11	4.225	−0.440	98.3	8.1	3.94	6.539	1.873	107.0	16.8
LC-BLYP	2.94	4.409	−0.364	89.6	3.0	4.30	6.535	1.762	103.4	16.9
ωB97XD	2.99	4.314	−0.459	89.6	3.2	4.32	6.556	1.784	103.5	17.0
M06-2X	3.42	4.573	−0.177	95.4	9.7	4.45	6.434	1.685	101.1	15.4
CASSCF	3.69	4.319	−0.108			4.72	4.911	0.484		
CASPT2	3.50	4.307	−0.115			4.48	5.295	0.873		
CC2	3.21					4.56				
CCSD	2.86	4.425	−0.100			4.42	6.210	1.685		
CCSD(T)		4.296	−0.187				6.030	1.547		

Relaxed geometries have been obtained with PBE0 using the aug-cc-pVTZ basis sets

3.3 Electric properties of the excited states of BN in the gas phase

Available experimental gas-phase μ values for the 1^1B state of BN come from the analysis of thermochromic shifts of absorption/fluorescence spectra by Kawski et al. [16] and from the Stark effect studies of the rotationally resolved fluorescence spectra by Borst et al. [15]. The former relies on the Onsager model in which known ground-state properties such as μ and α (enabling to estimate the Onsager interaction radius) are used to express the dependence of the excited-state dipole moment on the thermochromic shifts of absorption/fluorescence peaks. Using the ground-state μ_g value 4.18 D [60] for the analysis of the

fluorescence shifts, Kawski et al. obtained the excited-state value 4.42 D, corresponding to the excess dipole moment value $\Delta\mu = \mu_e - \mu_g = 0.24$ D, which was in a qualitative agreement with the value 0.31 D from an earlier UV studies [68, 69]. However, as we mentioned earlier, there are more recent measurements of μ_g of BN available. Therefore, rather than using Kawski's excited-state value, we compare our theoretical adiabatic excess dipole moment value to the Stark effect data obtained by Borst et al. [15] that lead to the ground-state μ_g value 4.48 D (in very good agreement with the value reported by Wohlfart et al. [59]) and the excited-state value 4.57 ± 0.01 D, which gives the excess dipole moment value $\Delta\mu = \mu_e - \mu_g = 0.09$ D. It is also worth noting that Kawski et al. observed only negligible thermochromic shifts of the absorption peaks in the region of 36,000–38,000 cm^{-1} (4.4–4.7 eV), suggesting that the 1^1B state has a negligible or at least very small vertical excess dipole moment value. In our further discussion, we compare the experimental data derived from fluorescence spectra with the adiabatic excess properties (using thus the excited-state equilibrium geometries), while the evidence from absorption spectra measurements are discussed in the context of the vertical excess properties (using thus the ground-state equilibrium geometries).

From Table 2, it can be seen that our CCSD vertical excess dipole moment value ($\Delta\mu_{vertical}$) of the 1^1B state is very small (0.046 D) in line with Kawski's observation. While the CC2 value is in a reasonable agreement with CCSD, hybrid and LRC-DFT methods give $\Delta\mu_{vertical}$ in the range of 0.21–0.28 D. Proximity of the BLYP and CCSD values should be considered as a coincidence, since the agreement is not repeated in case of other states. Let us notice that the CASSCF and CASPT2 dipole moment values are in a reasonable agreement with the CC methods here. This is, however, not the case of the 2^1A state. For this state, one can expect somewhat larger changes in the dipole moment due to the electron excitation, since its electron distribution gives rise to the quinoid structure when relaxed. Nevertheless, the π–π^* transition still occurs predominantly within the benzene ring, so $\Delta\mu_{vertical}$ should not be huge. In line with these expectations, the CCSD value is about 0.39 D being consistent with the CC2 result (0.37 D). The only DFT method giving $\Delta\mu_{vertical}$ with the sign consistent with CCSD is LC-BLYP. Other LRC-DFT approaches predicting $\Delta\mu_{vertical}$ −0.07 ± 0.01 D also appear to be closer to CCSD than the hybrids. However, the CASSCF and CASPT2 dipole moment values are noticeably out of the others, which put the reliability of the response approaches into question here. A more careful insight to the state-averaged CASSCF results suggests that there are in fact two close lying (within 0.5 eV) $^1A_1$ excited states with an important role of double excitations, which are not revealed by the response approaches. The dipole moments of these two states significantly differ (the vertical state-averaged CASSCF values are 2^1A_1: 7.3 D, 3^1A_1: 2.4 D). Moreover, the geometry relaxation results in the change in the ordering of the two states which leads to a qualitative change in the CASSCF dipole moment values (adiabatic values: 2^1A_1: 3.5 D, 3^1A_1: 6.3 D)—see further. We note that also Sobolewski et al. [42] obtained dipole moment value 7.1 D for 2^1A_1 using the ground-state geometry.

The $\Delta\mu$ values (formally referred to as "vertical" also for triplet states) for the 1^3A state (Table 3) are consistently predicted to be negative by all applied DFT- and WF-based approaches with the exception of the CASPT2 method. A comparison of the CCSD and CCSD(T) reveals that the (non-iterative) contribution of triple excitations is 0.09 D. Although DFT methods overestimate the decrease in μ, LRC-DFT values are in general closer to the CC results. Among hybrids, the M06-2X functional performs very well. Contrary to the 1^3A state, $\Delta\mu_{vertical}$ for the 1^3B state was found to be positive. DFT results are in this case in a fair agreement with the CCSD(T) value, which is about 1.34 D.

Adiabatic excess properties derived from excited-state properties evaluated in the optimized excited-state geometries obtained at the PBE0/*aug*-cc-pVTZ level are summarized in Tables 4 and 5. Let us note that we have also investigated a possible influence of the small changes in excited-state geometries on the properties by evaluating the adiabatic excited-state dipole moment and average polarizability in geometries optimized at the B3LYP/*aug*-cc-pVTZ level. We have observed negligible differences in our results (the maximum differences for μ and α_{av} have been observed for the 2^1A state: 0.017 D and 1.3 a.u., respectively). Adiabatic excess dipole moment values ($\Delta\mu_{adiabatic}$) for the 1^1B state reported in Table 4 are systematically larger than their vertical counterparts by about 0.06 (0.10) D at the CCSD (LRC-DFT) level in line with larger fluorescence shift compared with the absorption observed in experiment. Our CCSD value of $\Delta\mu_{adiabatic}$ equal to 0.11 D is in excellent agreement with the experimental value reported by Borst et al. [15], although one should keep in mind a possible source of error (ca. 0.05 D) due to the excited-state relaxation effects discussed above. The CASSCF and CASPT2 methods predict slightly smaller (by ca. 0.25 D) dipole moment for this excited state than CCSD. On the other hand, as in the vertical case, the hybrid and LRC-DFT methods exceed the CCSD $\Delta\mu_{adiabatic}$ value by about 0.24–0.26 D. The discrepancies between CC and DFT results in predicting the $\Delta\mu_{vertical}$ values of the 2^1A state are more pronounced in $\Delta\mu_{adiabatic}$ calculations. While CCSD predicts the increase in the excited-state dipole moment with respect to the ground state by 0.365 D, most of DFT as well anticipate the opposite change in the same magnitude. The LRC-DFT approaches are in line with the hybrids, although in a smaller extent. The CASSCF and

CASPT2 methods also predict $\Delta\mu_{adiabatic}$ with an opposite sign to the CCSD value; nevertheless, the differences between the total $\mu_{adiabatic}$ values obtained with the CAS and CC methods for this excited state are smaller compared with the vertical case. It can be noticed that Zilberg and Haas [41] also predict negative $\Delta\mu_{adiabatic}$ values (−0.1 and −0.5 D, respectively) for both 1^1B and 2^1A states at the CASSCF level, although they have used smaller active space (8,8) and smaller basis set (DZV).

Table 5 shows that using the excited-state optimized geometries in calculations of $\Delta\mu_{adiabatic}$ for the 1^3A (1^3B) states brings about decrease (increase) in the $\Delta\mu$ compared with their vertical counterparts by about 0.1 D (0.3 D). Like in the vertical calculations, LRC-DFT $\Delta\mu_{adiabatic}$ values are in general closer to the CC results than those obtained with other DFT methods. Among hybrids, M06-2X again performs very well.

In Tables 2 and 3, one can also observe changes in α due to the vertical electron excitation. In line with the structure and dipole moment analyses, the excess polarizability values $\Delta\alpha_{vertical}$ are much smaller for the 1^1B state (as a locally excited state) compared with the 2^1A state. Considering the CCSD results as the most accurate for the singlet states, the increase in polarizability with respect to the ground state is about 7 % (46 %) for the former (latter). In this context, the assumption of the similar polarizability values of the 1^1A and 1^1B states of BN by Kawski et al. in their study can be considered reasonable. In case of the 1^1B state, all applied DFT methods slightly exceed the CCSD value ($\Delta\alpha_{vertical} = 6.4$ a.u.). While LRC-DFT together with the M06-2X functional and CC2 gives the values in the range of 9–12 a.u., pure and hybrid DFTs' overestimations are larger. The 2^1A state appears to be more sensitive to selected method. The predictions of hybrids are now closer to CCSD, while LRC-DFTs underestimate the CCSD value ($\Delta\alpha_{vertical} = 39.8$ a.u.) by about 13 a.u. Although for the triplet states we do not have CC reference values, one can see that DFT results are fairly consistent enabling us to draw at least semiquantitative conclusions. Firstly, one can observe very small (almost negligible) $\Delta\alpha_{vertical}$ values for the 1^3A state. Deeper analysis of the $\Delta\alpha_{vertical}$ components reveals that the increase in the α_{zz} component (by about 7 a.u.) is effectively compensated by the decrease in the α_{xx} component. Anyway, the large difference between the $\Delta\alpha_{vertical}$ (but also $\Delta\mu_{vertical}$) values for the 1^1A and 1^3A states suggests that the spin state can have a significant impact on electric properties of "otherwise similar" electronic states. The differences in excess polarizability values between the states can be explained in terms of the of the sum-over-states description for the polarizability:

$$\alpha_i = \frac{2}{3}\sum_{n\neq i}\frac{|\mu_{ni}|^2}{\Delta E_{ni}} \quad (1)$$

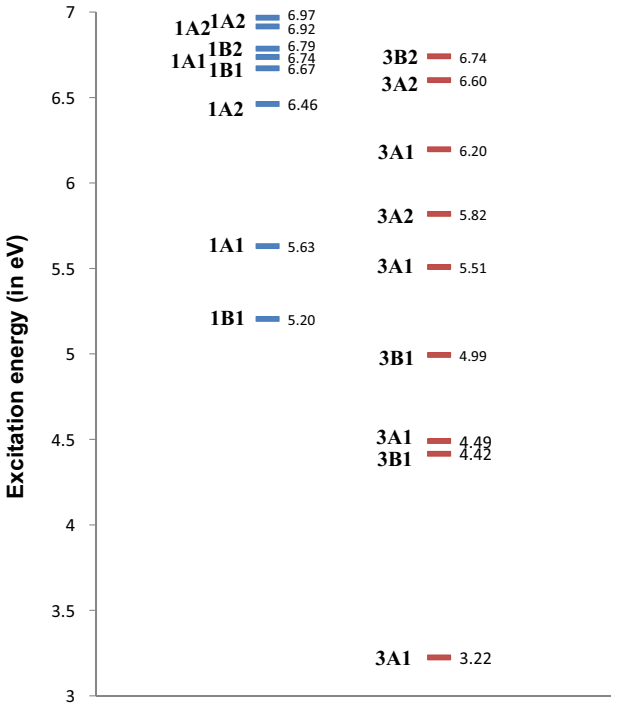

Fig. 3 Schematic energy level diagram for the singlet and triplet states of BN calculated at the TD-CAM-B3LYP/POL level

where i is the state of interest, ΔE_{ni} is the energy difference between states i and n and μ_{ni} is the corresponding transition dipole moment. It can be seen in Fig. 3 that contrary to the two lowest singlet states and also contrary to the 1^3B ($^3B_1$) state, the $^3A_1$ state is far below the $^3B_1$ state (by 1.2 eV). Although the complete analysis would require consideration of more states and evaluating the transition moments, the large qualitative differences in excited energies of the most important states indicate that one can expect the particular behavior of the $^3A_1$ state.

Using the excited-state optimized geometries in calculations of $\Delta\alpha_{adiabatic}$ for the lowest singlet and triplet states brings only minor changes (typically less than 2–3 a.u.) compared with their vertical counterparts. As expected, the most sensitive quantity is $\Delta\alpha_{adiabatic}$ for the 2^1A state. While its decrease due to the geometry relaxation is predicted to be only about 3 a.u. by CCSD, LRC-DFTs and hybrid DFTs predict the decrease by about 10–12 a.u., which can be considered as semiquantitatively correct estimates.

3.4 Solvent effects on the ground-state properties

Before discussing excited-state properties, let us firstly describe impact of solvation on the ground-state μ and α. Contrary to excited states here the general methodology is well established and tested [47–49] against experimental values, although we recall again that in case of solvents for

which specific solute–solvent interactions (such as hydrogen bonding) it is necessary to turn to explicit solvent models. Adding solvent effects by means of continuum solvation model leads in case of BN to increase in both dipole moment as well as all components of α (see Table 6). The increase in μ can be explained as follows: Partial charges on BN molecule induce opposite charges on cavity surface and both are equilibrated until self-consistency is achieved, which leads to more polarized electron density. Solvation by nonpolar cyclohexane increases dipole moment significantly by 11 % (0.56 D) compared with the gas phase. Further increase is observed in more polar solvents (see Fig. 4) leading to the μ_g value of 6.18 D in water compared with 4.79 D in the gas phase. The same trend was observed for α: With increasing polarity function of selected solvents α increases. We obtained 12 % increase in average polarizability (α_{av}) by moving from the gas phase to cyclohexane. Water as the most polar from used solvents increases average polarizability to 117.8 a.u. compared with gas-phase value 86.4 a.u. While there are no experimental results for dipole moments, solvent effects on electronic polarizability of BN were measured by Alvarado et al. [63] in several solvents (cyclohexane, CCl_4, tetrahydrofuran, acetonitrile). Using measurements of refraction index of diluted solutions, they found no dependence of static α on solvent polarity. For cyclohexane, the experimental value is 83.7 a.u., then it slightly decreases to 81.5 a.u. (CCl_4), and the value in polar acetonitrile is 82.3 a.u. Unclear trends of static polarizability on solvent polarity were also found in other experimental works studying methylthiophenes [70] and pyrazabole [71]. Possible explanation of the discrepancy in the trend between theory and experiment can lie in insufficient treatment of specific interactions and dispersion (or more generally non-electrostatic) interactions and between solvent molecules and solute, since the PCM model is mainly electrostatic model (comparable situation was found in, e.g., [72]). We note that while for higher frequencies the experimental dynamic polarizability of BN in acetonitrile is the largest from studied solvents, when approaching static limit it becomes smaller than values in cyclohexane and tetrahydrofuran. This supports our conclusion that more sophisticated approaches taking also solvent–solute dispersion interactions are needed for reproducing the experimental results in solvents.

3.5 Solvent effects on excitation energies and properties of excited states

Since we limit our discussion to vertical excitations, the non-equilibrium model was used in connection with LR and cLR methods to account for the solvation effects on excited-state properties as described in Computational Details. Excitation energies for the first singlet excited state (1^1B) are slightly red-shifted according to our calculations when going from gas phase to nonpolar solvent as a cyclohexane (−0.013 eV at cLR level). Larger red shift (−0.024 eV) was obtained when using only transition density to model the change in electron density in excited state (LR). This shift is even pronounced in more polar solvents. These results are in line with our results for $\Delta\mu_{vertical}$ in gas phase (e.g., $\Delta\mu_{vertical} = 0.27$ D at the CAM-B3LYP level). For the 2^1A, $\Delta\mu_{vertical}$ in gas phase is almost negligible (decrease by 0.08 D), which is also reflected by almost constant cLR excitation energy (changes are less than 0.004 eV) for this state independently on solvent used. Excitation to 2^1A is symmetry allowed (oscillator strength $f = 0.21$) and thus has large transition dipole moment (corresponding to respective transition density) which generates red solvent shift of 0.07 eV in case of the LR method.

The change in the dipole moment due to electron excitation is frequently used for predicting red/blue solvent shifts of electron absorption/emission spectra and vice versa, the backward analysis of these spectra is used for calculation of dipole moments. Standard assumption is that the excess of dipole moment remains constant in larger sequence of solvents. In Table 6 and Fig. 4, one can find that the excited-state dipole moment values grow more steeply than for ground state. Steepest is the increase for 1^3B followed by 2^1A and 1^1B, while the change in $\Delta\mu$ for 1^3A state is negligible with respect to the solvent polarity. Very interesting is the situation for the 2^1A state, where the excited-state dipole moment is slightly smaller than that of the ground state (difference −0.076 D at the CAM-B3LYP level) in gas phase, but after solvation by nonpolar cyclohexane the situation is reversed, and in the water, $\Delta\mu$ is even equal to 1.042 D.

Solvent effects on α of the BN molecule in its excited states were evaluated using both LR and cLR methods. Although there is a lot of evidence concerning performance of cLR method (or in general state specific solvation models) for excitation energies calculations [73–76], only limited number of studies use cLR solvation model also for modeling of electric properties of excited states [77]. It can be seen from the results in Table 6 (and Fig. 5) that $\Delta\alpha$ increases with increasing solvent polarity for 1^1B, 2^1A and 1^3B. This means that more diffuse electron density of excited states responds stronger in more polar solvents than the ground-state density. For example, while $\Delta\alpha$ is 12.2 a.u. for the 1^1B excited state in the gas phase, it approaches 22 a.u. in acetone. In the case of the 1^3A state, the polarizability is only slightly smaller than that in the ground state (by ca. 1 a.u.), and the difference remains almost constant for both LR and cLR approaches as the solvent polarity increases. Our qualitative analysis of the gas-phase values of α for the 1^3A state based on the SOS theory can be extended here to suggest a possible explanation of

Table 6 Solvent effects on vertical excitation energies (in eV), dipole moment (in D) and polarizability (in a.u.) of the ground state and low-lying singlet and triplet excited states of benzonitrile obtained with CAM-B3LYP using Sadlej's POL basis sets

Solvent data			GS	1^1B		2^1A		1^3A		1^3B	
Solvent[a]	ε	$1-1/\varepsilon$		LR	cLR	LR	cLR	LR	cLR	LR	cLR
Excitation energy											
GAS	1.00	0.000		5.205		5.630		3.225		4.416	
CHX	2.02	0.505		5.181	5.191	5.560	5.632	3.239	3.237	4.368	4.346
ETA	5.99	0.833		5.167	5.175	5.563	5.628	3.251	3.250	4.322	4.296
DCM	8.93	0.888		5.162	5.171	5.554	5.627	3.254	3.252	4.313	4.283
ACT	20.70	0.952		5.160	5.167	5.561	5.625	3.257	3.255	4.302	4.274
Dipole moment											
GAS	1.00	0.000	4.791	5.061	5.061	4.714	4.714	4.418	4.418	6.190	6.190
CHX	2.02	0.505	5.353	5.930	5.912	5.668	5.658	4.987	4.984	7.152	7.277
ETA	5.99	0.833	5.871	6.825	6.723	6.662	6.616	5.521	5.521	8.078	8.230
DCM	8.93	0.888	5.973	7.018	6.903	6.875	6.827	5.630	5.630	8.268	8.446
ACT	20.70	0.952	6.100	7.257	7.107	7.142	7.069	5.762	5.762	8.502	8.678
Mean dipole polarizability											
GAS	1.00	0.000	86.4	98.6	98.6	113.9	113.9	86.3	86.3	105.1	105.1
CHX	2.02	0.505	97.4	113.0	113.0	131.5	133.9	97.0	97.2	119.5	119.7
ETA	5.99	0.833	109.0	129.5	128.0	151.3	153.1	108.7	109.3	136.5	137.0
DCM	8.93	0.888	112.1	133.2	132.7	155.8	158.2	111.4	111.9	140.4	141.6
ACT	20.70	0.952	115.6	138.1	137.6	161.6	163.5	114.8	115.2	145.5	146.4

[a] *GAS* gas phase, *CHX* cyclohexane, *ETA* ethyl acetate, *DCM* dichloromethane, *ACT* acetone

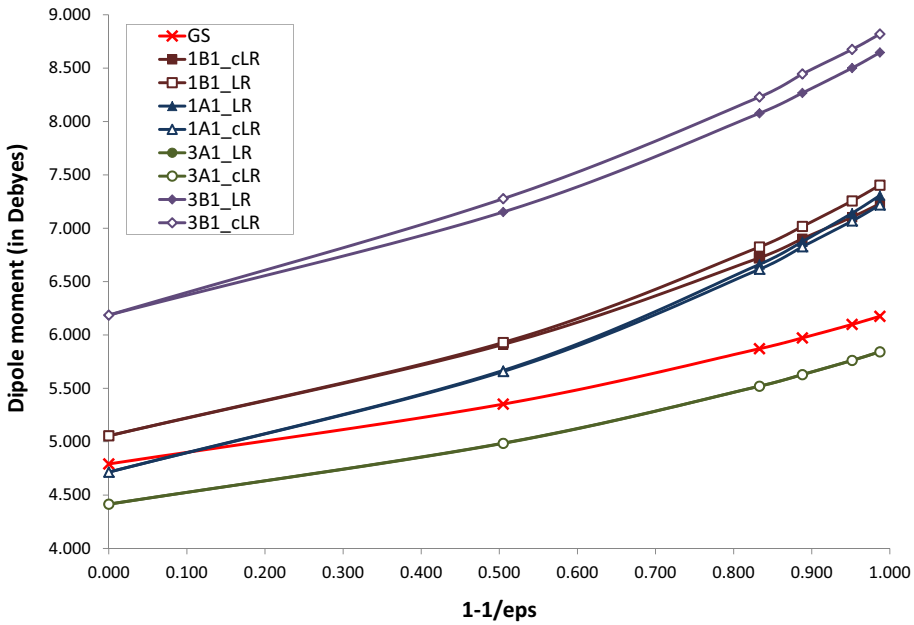

Fig. 4 Dependence of the dipole moment on the solvent polarity evaluated for the ground and lowest excited states of benzonitrile at the CAM-B3LYP/POL level using the LR and cLR PCM models to account for the solvent effects

this observation. It can be seen in Table 6 that contrary to other states the excitation energy of the 1^3A state slightly increases with the solvent polarity partly compensating the anticipated increase in the transition dipole moment.

From a methodological point of view, it is interesting to observe that the LR and cLR approaches provide very similar results for both investigated singlet states, i.e., almost independently on whether the corresponding transition is symmetry allowed or not. The difference on the average polarizability between the two approaches for the 2^1A state is only about 2 %, and the difference appears to be independent on solvent polarity. This observation can possibly be explained by the local character of the studied excitations which lead to rather small excess dipole moment

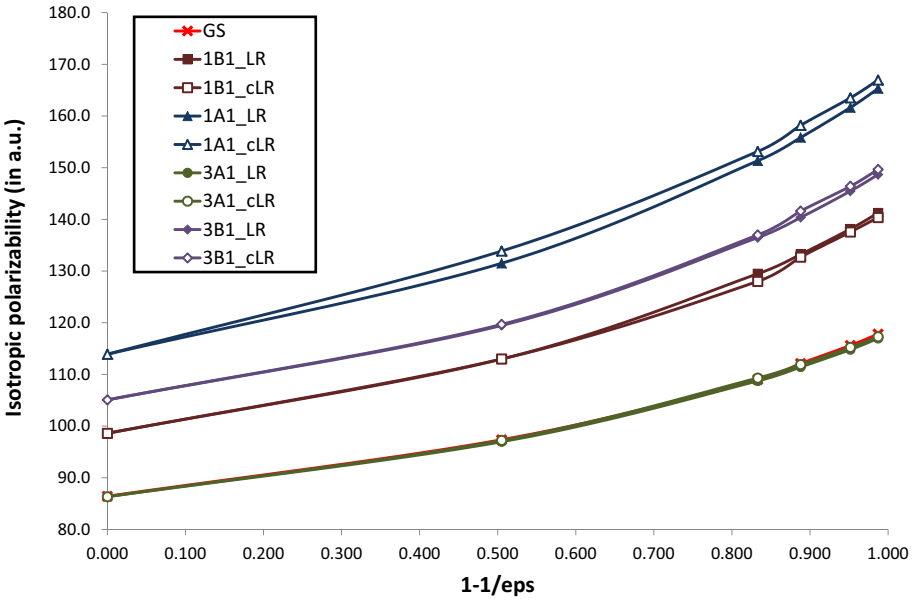

Fig. 5 Dependence of the isotropic polarizability on the solvent polarity evaluated for the ground and lowest excited states of benzonitrile at the CAMB3LYP/POL level using the LR and cLR PCM models for the solvent effects

values resulting in small changes in apparent charges on the cavity due to the excitations. Therefore, it is not so important whether we use the transition densities (LR) or the one-particle TD-DFT density matrix (cLR) to account for the impact of excitation on the cavity charge distribution.

4 Conclusions

A variety of WF- and DFT-based methods has been used to obtain accurate μ and α values for the ground and lowest singlet (1^1B and 2^1A) and triplet (1^3A and 1^3B) excited states of BN.

For the ground state, a comparison of our theoretical results to the experimental values shows excellent performance of both CCSD and CCSD(T) methods, but also MP2. Hybrid and LRC-DFT methods slightly overshoot (by about 0.20–0.25 D) the μ_g value. In the context of the comparison with experiment, we also estimated the error in experimental measurements due to the excited-state relaxation effects to be about 0.05 D. To our best knowledge, the gas-phase value of α_{av} of BN is not known experimentally. Our estimate obtained at the CCSD(T) level is 84.73 a.u. Both hybrid and LRC-DFT methods are in fair agreement with this reference value.

The two lowest singlet excited states have the local π–π^* character. The lowest excited state is 1^1B, and it corresponds to the electron excitation from the HOMO-1 to the LUMO. The second excited state is the 2^1A symmetry, and although it can be predominantly described as the electron excitation from the HOMO to the LUMO, it has a partial double-excitation character, which is moreover sensitive to geometrical changes. Conversely, the two lowest triplet states show up the reverse ordering, i.e., the 1^3A state is energetically lower than the 1^3B state. In all the examined excited states, the molecule retains the C_{2v} symmetry. While in the 1^1B state the benzene ring remains essentially a perfect hexagon (as in the ground state), the 2^1A state has quinoid structure. The structures of the triplet states are similar to their singlet counterparts with more pronounced quinoid character of the 1^3A state.

The change in a property due to the electron excitations is referred to as the excess of the property for a particular excited state. Our CCSD vertical excess dipole moment value $\Delta\mu_{vertical}$ for the 1^1B state is very small (0.046 D) in line with experimental observation. While the CC2 value is in a reasonable agreement with CCSD, all hybrid and LRC-DFT methods overestimate this value (0.21–0.28 D). For the 2^1A state, the CCSD $\Delta\mu_{vertical}$ value is about 0.39 D. The only DFT method giving the same sign is LC-BLYP. Large difference between the CASPT2 and CCSD results suggests that the predictions of $\Delta\mu_{vertical}$ value for this state obtained by response approaches should be taken with caution. The $\Delta\mu$ values for the triplet state are consistently predicted to be negative by all applied DFT- and WF-based approaches. Although DFT methods overestimate the decrease in the dipole moment, LRC-DFT values are in general closer to the CC results.

Adiabatic excess dipole moment values for the 1^1B state are systematically larger than their vertical counterparts by about 0.06 D in line with larger fluorescence shift compared with the absorption observed in experiment. Our CCSD value of $\Delta\mu_{adiabatic}$ equal to 0.11 D is in excellent agreement with the experimental value reported by Borst et al. [15]. The performance of DFT methods compared with CCSD is effectively the same as in the case of vertical values.

In line with the structure and dipole moment analyses, $\Delta\alpha_{\text{vertical}}$ is much smaller (CCSD: 7 %) for the 1^1B state compared with the 2^1A state (CCSD: 46 %). In case of the 1^1B state, all applied DFT methods slightly exceed the CCSD value. The 2^1A state appears to be more sensitive to selected method, probably due to a more important role of double-excitation effects revealed by the CASSCF method. Although for the triplet states we do not report CC reference values, one can see that DFT results are fairly consistent. Using the excited-state optimized geometries in calculations of $\Delta\alpha_{\text{adiabatic}}$ for the lowest singlet and triplet states brings only minor changes compared with their vertical counterparts.

To summarize, the performance of the applied hybrid and LRC-DFT methods in the excited-state property calculations for local π–π^* transitions in BN was found to be fairly reasonable being able to semiquantitatively capture the main differences between the studied states. The most consistent results with those provided by the CC methods were obtained with LC-BLYP. Nevertheless, the determination of the excess properties particularly for the singlet states with a partial double-excitation character appeared to be rather problematic for the used DFT methods. Of course, more evidence is definitely needed to draw more general conclusions on applicability of DFT methods for evaluation of excited-state properties of medium-sized molecules.

Solvent effects on μ and α of the BN molecule in its ground and excited states were evaluated using both LR and cLR methods combined with the (TD-)CAMB3LYP/POL approach. In line with the calculated $\Delta\mu_{\text{vertical}}$, the excitation energies for the 1^1B state are slightly red-shifted when going from the gas phase to nonpolar solvent. This shift is even more pronounced in polar solvents. For the 2^1A state, $\Delta\mu_{\text{vertical}}$ in gas phase is almost negligible, which is reflected by almost constant cLR excitation energy for this state independently on solvent used. We found that the excited-state dipole moments grow more steeply than for ground state. We also observed that $\Delta\alpha$ increases with increasing solvent polarity for 1^1B, 2^1A and 1^3B, which was explained in terms of the more diffuse electron density of excited states compared with the ground-state density. Finally, we note that in property calculations we observed consistent performance of LR and computationally more demanding cLR approaches.

Acknowledgments This work has been supported by the project "Mobilities - enhancing research, science and education at the Matej Bel University," ITMS code: 26110230082, under the Operational Program Education financed by the European Social Fund. Part of the computations was performed in the HPC Centers of the Matej Bel University in Banská Bystrica and the Slovak Academy of Sciences in Žilina using the HPC infrastructure acquired in project ITMS 26230120002 and 26210120002 (Slovak infrastructure for high-performance computing) supported by the Research & Development Operational Programme funded by the ERDF. T.P. acknowledges the computational grants from the Supercomputer and Networking Center ACK CYFRONET AGH in Krakow, Poland (MNiSW/Zeus_lokalnie/UŚląski/011/2014), and from the Wroclaw Centre for Networking and Supercomputing, in Wrocław, Poland.

References

1. Prasad PN, Williams DJ (1991) Introduction to nonlinear optical effects in molecules and polymers. Wiley, New York
2. Kanis DR, Ratner MA, Marks TJ (1994) Chem Rev 94:195–242
3. She CX, Easwaramoorthi S, Kim P, Hiroto S, Hisaki I, Shinokubo H, Osuka A, Kim D, Hupp JT (2010) J Phys Chem A 114:3384–3390
4. Urban M, Sadlej AJ (1990) Theor Chim Acta 78:189–201
5. Klein S, Kochanski E, Strich A, Sadlej AJ (1996) Theor Chim Acta 94:75–91
6. Palenikova J, Kraus M, Neogrady P, Kello V, Urban M (2008) Mol Phys 106:2333–2344
7. Pasteka LF, Melichercik M, Neogrady P, Urban M (2012) Mol Phys 110:2219–2237
8. Bublitz GU, Boxer SG (1997) Annu Rev Phys Chem 48:213–242
9. Boxer SG (2009) J Phys Chem B 113:2972–2983
10. Premvardhan LL, Peteanu LA (2002) J Photochem Photobiol A 154:69–79
11. Casida ME, Huix-Rotllant M (2012) Annu Rev Phys Chem 63:287–323
12. Pluta T, Kolaski M, Medveď M, Budzak S (2012) Chem Phys Lett 546:24–29
13. Grozema FC, Telesca R, Jonkman HT, Siebbeles LDA, Snijders JG (2001) J Chem Phys 115:10014–10021
14. Grozema FC, Telesca R, Snijders JG, Siebbeles LDA (2003) J Chem Phys 118:9441–9446
15. Borst DR, Korter TM, Pratt DW (2001) Chem Phys Lett 350:485–490
16. Kawski A, Kuklinski B, Bojarski P (2006) Chem Phys Lett 419:309–312
17. Demeter A, Zachariasse KA (2008) J Phys Chem A 112:1359–1362
18. Becke AD (1988) Phys Rev A 38:3098–3100
19. Lee CT, Yang WT, Parr RG (1988) Phys Rev B 37:785–789
20. Becke AD (1993) J Chem Phys 98:1372–1377
21. Stephens PJ, Devlin FJ, Chabalowski CF, Frisch MJ (1994) J Phys Chem-Us 98:11623–11627
22. Adamo C, Barone V (1999) J Chem Phys 110:6158–6170
23. Yanai T, Tew DP, Handy NC (2004) Chem Phys Lett 393:51–57
24. Chai JD, Head-Gordon M (2008) J Chem Phys 128:084106
25. Tawada Y, Tsuneda T, Yanagisawa S, Yanai T, Hirao K (2004) J Chem Phys 120:8425–8433
26. Zhao Y, Truhlar DG (2008) Theor Chem Acc 120:215–241
27. Roos BO (2007) The complete active space self-consistent field method and its applications in electronic structure calculations. Adv Chem Phys. doi:10.1002/9780470142943
28. Andersson K, Malmqvist PA, Roos BO, Sadlej AJ, Wolinski K (1990) J Phys Chem 94:5483–5488
29. Andersson K, Malmqvist PÅ, Roos BO (1992) J Chem Phys 96:1218–1226
30. Dunning TH (1989) J Chem Phys 90:1007–1023
31. Guido CA, Jacquemin D, Adamo C, Mennucci B (2010) J Phys Chem A 114:13402–13410
32. Sadlej AJ (1988) Collect Czechoslov Chem Commun 53:1995–2016
33. Benkova Z, Cernusak I, Zahradnik P (2006) Mol Phys 104:2011–2026

34. Jacquemin D, Wathelet V, Perpete EA, Adamo C (2009) J Chem Theory Comput 5:2420–2435
35. Iikura H, Tsuneda T, Yanai T, Hirao K (2001) J Chem Phys 115:3540–3544
36. Silva MR, Schreiber M, Sauer SPA, Thiel W (2008) J Chem Phys 129:104103
37. Jacquemin D, Perpete EA, Ciofini I, Adamo C, Valero R, Zhao Y, Truhlar DG (2010) J Chem Theory Comput 6:2071–2085
38. Christiansen O, Halkier A, Koch H, Jorgensen P, Helgaker T (1998) J Chem Phys 108:2801–2816
39. Aidas K, Angeli C, Bak KL, Bakken V, Bast R, Boman L, Christiansen O, Cimiraglia R, Coriani S, Dahle P, Dalskov EK, Ekstrom U, Enevoldsen T, Eriksen JJ, Ettenhuber P, Fernandez B, Ferrighi L, Fliegl H, Frediani L, Hald K, Halkier A, Hattig C, Heiberg H, Helgaker T, Hennum AC, Hettema H, Hjertenaes E, Host S, Hoyvik IM, Iozzi MF, Jansik B, Jensen HJA, Jonsson D, Jorgensen P, Kauczor J, Kirpekar S, Kjrgaard T, Klopper W, Knecht S, Kobayashi R, Koch H, Kongsted J, Krapp A, Kristensen K, Ligabue A, Lutnaes OB, Melo JI, Mikkelsen KV, Myhre RH, Neiss C, Nielsen CB, Norman P, Olsen J, Olsen JMH, Osted A, Packer MJ, Pawlowski F, Pedersen TB, Provasi PF, Reine S, Rinkevicius Z, Ruden TA, Ruud K, Rybkin VV, Salek P, Samson CCM, de Meras AS, Saue T, Sauer SPA, Schimmelpfennig B, Sneskov K, Steindal AH, Sylvester-Hvid KO, Taylor PR, Teale AM, Tellgren EI, Tew DP, Thorvaldsen AJ, Thogersen L, Vahtras O, Watson MA, Wilson DJD, Ziolkowski M, Agren H (2014) Wires Comput Mol Sci 4:269–284
40. Christiansen O, Koch H, Jorgensen P (1995) Chem Phys Lett 243:409–418
41. Zilberg S, Haas Y (2002) J Phys Chem A 106:1–11
42. Sobolewski AL, Domcke W (1996) Chem Phys Lett 250:428–436
43. Rutishauser H (1963) Matematik 5:48–54
44. Medved M, Stachova M, Jacquemin D, Andre JM, Perpete EA (2007) J Mol Struct Theochem 847:39–46
45. Amovilli C, Barone V, Cammi R, Cances E, Cossi M, Mennucci B, Pomelli CS, Tomasi J (1999) Adv Quantum Chem 32:227–261
46. Tomasi J, Mennucci B, Cammi R (2005) Chem Rev 105:2999–3093
47. Cammi R, Mennucci B, Tomasi J (2000) J Phys Chem A 104:4690–4698
48. Illien B, Evain K, Le Guennec M (2003) J Mol Struct Theochem 630:1–9
49. Benassi E, Egidi F, Barone V (2015) J Phys Chem B 119:3155–3173
50. Sylvester-Hvid KO, Mikkelsen KV, Norman P, Jonsson D, Ågren H (2004) J Phys Chem A 108:8961–8965
51. Cammi R, Mennucci B (1999) J Chem Phys 110:9877–9886
52. Cossi M, Barone V (2001) J Chem Phys 115:4708–4717
53. Caricato M, Mennucci B, Tomasi J, Ingrosso F, Cammi R, Corni S, Scalmani G (2006) J Chem Phys 124:124520
54. Schmidt MW, Baldridge KK, Boatz JA, Elbert ST, Gordon MS, Jensen JH, Koseki S, Matsunaga N, Nguyen KA, Su SJ, Windus TL, Dupuis M, Montgomery JA (1993) J Comput Chem 14:1347–1363
55. Gordon MS, Schmidt MW (2005) Chapter 41: advances in electronic structure theory: GAMESS a decade later. In: Dykstra CE, Frenking G, Kim KS, Scuseria GE (eds) Theory and applications of computational chemistry. Elsevier, Amsterdam, pp 1167–1189. doi:10.1016/B978-044451719-7/50084-6
56. Frisch MJ, Trucks GW, Schlegel HB, Scuseria GE, Robb MA, Cheeseman JR, Scalmani G, Barone V, Mennucci B, Petersson GA, Nakatsuji H, Caricato M, Li X, Hratchian HP, Izmaylov AF, Bloino J, Zheng G, Sonnenberg JL, Hada M, Ehara M, Toyota K, Fukuda R, Hasegawa J, Ishida M, Nakajima T, Honda Y, Kitao O, Nakai H, Vreven T, Montgomery Jr. JA, Peralta JE, Ogliaro F, Bearpark MJ, Heyd J, Brothers EN, Kudin KN, Staroverov VN, Kobayashi R, Normand J, Raghavachari K, Rendell AP, Burant JC, Iyengar SS, Tomasi J, Cossi M, Rega N, Millam NJ, Klene M, Knox JE, Cross JB, Bakken V, Adamo C, Jaramillo J, Gomperts R, Stratmann RE, Yazyev O, Austin AJ, Cammi R, Pomelli C, Ochterski JW, Martin RL, Morokuma K, Zakrzewski VG, Voth GA, Salvador P, Dannenberg JJ, Dapprich S, Daniels AD, Farkas Ö, Foresman JB, Ortiz JV, Cioslowski J, Fox DJ (2009) Gaussian 09 A.1. Gaussian, Inc., Wallingford, CT
57. Aquilante F, De Vico L, Ferré N, Ghigo G, Malmqvist PÅ, Neogrády P, Pedersen TB, Pitoňák M, Reiher M, Roos BO, Serrano-Andrés L, Urban M, Veryazov V, Lindh R (2010) J Comput Chem 31:224–247
58. Lide DR (1954) J Chem Phys 22:1577–1578
59. Wohlfart K, Schnell M, Grabow JU, Kupper J (2008) J Mol Spectrosc 247:119–121
60. Lide DR (ed) (1993) Handbook of chemistry and physics, 73rd edn. CRC Press, Boca Raton
61. Le Fevre CG, Le Fevre RJW (1954) J Chem Soc 1954:1577–1588
62. Le Fevre RJW, Orr BJ, Ritchie GLD (1965) J Chem Soc 1965:2499–2505
63. Alvarado YJ, Labarca PH, Cubillan N, Osorio E, Karam A (2003) Z Naturforsch A 58:68–74
64. Peach MJG, Benfield P, Helgaker T, Tozer DJ (2008) J Chem Phys 128:044118
65. Reed AE, Weinstock RB, Weinhold F (1985) J Chem Phys 83:735–746
66. Borst DR, Pratt DW, Schaeffer M (2007) Phys Chem Chem Phys 9:4563–4571
67. Winter NOC, Graf NK, Leutwyler S, Hattig C (2013) Phys Chem Chem Phys 15:6623–6630
68. Huang KT, Lombardi JR (1971) J Chem Phys 55:4072–4076
69. Muirhead AR, Hartford A, Huang KT, Lombardi JR (1972) J Chem Phys 56:4385–4393
70. Alvarado YJ, Cubillan N, Labarca PH, Karam A, Arrieta F, Castellano O, Soscún H (2002) J Phys Org Chem 15:154–164
71. Alvarado YJ, Soscún H, Velazco W, Labarca PH, Cubillan N, Hernández J (2002) J Phys Org Chem 15:835–843
72. Mennucci B, Tomasi J, Cammi R, Cheeseman JR, Frisch MJ, Devlin FJ, Gabriel S, Stephens PJ (2002) J Phys Chem A 106:6102–6113
73. Chibani S, Budzak S, Medved M, Mennucci B, Jacquemin D (2014) Phys Chem Chem Phys 16:26024–26029
74. Chibani S, Laurent AD, Blondel A, Mennucci B, Jacquemin D (2014) J Chem Theory Comput 10:1848–1851
75. Jacquemin D, Chibani S, Le Guennic B, Mennucci B (2014) J Phys Chem A 118:5343–5348
76. Improta R, Barone V (2009) J Mol Struct Theochem 914:87–93
77. Budzak S, Medveď M, Mennucci B, Jacquemin D (2014) J Phys Chem A 118:5652–5656